Scientific Research Publishing

Engineering, 2018, 10, 187-201
http://www.scirp.org/journal/eng
ISSN Online: 1947-394X
ISSN Print: 1947-3931

Bromination of Pd Compounds during Thermal Decomposition of Tetrabromobisphenol A

Shunsuke Kuzuhara[1], Ayaka Sano[1,2]

[1]National Institute of Technology, Sendai College, Miyagi, Japan
[2]Senju Metal Industry Co., Ltd, Tokyo, Japan
Email: kuzuhara@sendai-nct.ac.jp

How to cite this paper: Kuzuhara, S. and Sano, A. (2018) Bromination of Pd Compounds during Thermal Decomposition of Tetrabromobisphenol A. *Engineering*, **10**, 187-201.
https://doi.org/10.4236/eng.2018.104013

Received: March 23, 2018
Accepted: April 27, 2018
Published: April 30, 2018

Abstract

We conducted thermal tests using the reagent tetrabromobisphenol A (TBBPA) and various Pd compounds to study the chemical forms of Pd obtained during the pyrolytic and oxidative decomposition of TBBPA. Thermal testing was conducted in an electric furnace at temperatures of 280˚C - 800˚C in an Ar or Ar-O_2 (5%) atmosphere for a heating period of 40 min. Scanning electron microscopy-energy dispersive X-ray spectroscopy results revealed that Pd bromide was formed in the mixture of TBBPA and PdO after heating to 450˚C in the Ar atmosphere. In addition, thermogravimetry-differential thermal analysis showed that as the heating temperature was increased from 350˚C to 730˚C, weight loss occurred at a nearly constant rate, indicating that Pd bromide decomposed in this temperature range.

Keywords

Tetrabromobisphenol A, Palladium, Waste Electrical and Electronic Equipment, Bromination, Thermal Processes

1. Introduction

Small electronic devices including mobile phones, laptop, digital cameras, and game consoles are essential in our daily lives, and the demand for these products is projected to increase. The increasing demand for small electronics will also lead to an increase in the generation of waste electrical and electronic equipment (WEEE). Approximately 4500 tonnes of WEEE is produced annually [1], and this quantity is projected to increase as developing countries grow.

Circuit boards in WEEE are highly valuable, since they contain metals including Cu, Ag, Au, and Pd [2] [3] [4]. Several metal recovery methods have been proposed, including pyrometallurgy [5], hydrometallurgy [6] [7] [8], bio-

technology [4] [9], and supercritical [10] [11] and high-voltage electrical pulse methods [12]. In particular, pyrometallurgy has been commercialised because of its potential for processing large volumes of materials [5]. From the perspective of metal quality, waste circuit boards rank higher than ores [13] and are suitable for recycling. However, they also contain flame retardants, which not only damage the equipment because of the halogens present within but also adversely affect metal recovery rates. Commonly used flame retardants include high impact polystyrene, acrylonitrile-butadiene-styrene, and tetrabromobisphenol A (TBBPA), with TBBPA being the most widely used.

The principal decomposition component in the thermolysis and pyrolysis of TBBPA is HBr [8] [14]; however, many organic compounds such as phenols and bromophenols are also formed [14]-[20]. The formation pathways [21] of polybrominated dibenzo-p-dioxins and dibenzofurans are still being studied.

Halogens are considered as aversive substances in metal recovery processes, with chloride volatilisation as an example of its positive use. By exploiting the chlorination reaction of metals [22] [23] [24], metal recovery can be in an energy-efficient manner; similarly, the bromination reaction of metals [25] can also be used. Basic information regarding the bromination reaction of metals is needed to increase the rate of metal recovery from waste circuit boards and prevent unintentional loss, and studies have been conducted using thermodynamic calculations [26]. Experimental quantitative analysis regarding the bromination behaviour of Zn has been conducted through thermal testing of samples containing ZnO and TBBPA [27] [28] [29]. Similar studies have been conducted for many other metals including PbO [30] [31], Fe_2O_3 [31], Sb_2O_3 [32], Cu [8], Ag [8], Au [8], and electric arc furnace dust [33].

In this study, we prepared samples and conducted thermal tests to study the chemical forms of metals observed during the thermal decomposition and combustion of TBBPA. Mixtures of TBBPA and Pd were prepared, and the TBBPA decomposition behaviour was studied by analysing the C and Br concentrations in solid samples and HBr emissions in the exhaust gas after thermal testing. Investigation of the chemical forms of Pd was primarily based on the results of crystal structure analysis using X-ray diffraction (XRD) and scanning electron microscopy-energy dispersive X-ray spectroscopy (SEM-EDS) elemental mapping images.

2. Experimental

2.1. Samples

The reagents Pd, PdO, $PdBr_2$, and TBBPA ($C_{15}H_{12}Br_4O_2$) were used to prepare the test samples. Sample mixtures of Pd and TBBPA and PdO and TBBPA were prepared in weight ratios of Pd:TBBPA 1:10.22 and PdO:TBBPA 1:8.89, respectively, and were subjected to thermal testing in an electric furnace. Granular samples were fabricated by subjecting the pulverised mixtures to a pressure of 12 MPa for 30 min to form shapes with dimensions of φ = 5 mm and h = 21 mm. In

this study, the two prepared mixtures were referred to as Pd + TBBPA and PdO + TBBPA.

2.2. Thermogravimetry-Differential Thermal Analysis Measurements

Thermogravimetry-differential thermal analysis (TG-DTA) measurements of the sample mixtures were also performed (Rigaku Co., Ltd. Thermo Plus TG 8120 analyser). First, a 10 mg sample was packed in a 2.5-mm-diameter alumina boat and heated from room temperature to 1000˚C at a rate of 10˚C/min under a He or an Ar-O_2 (5 mol%) environment at 100 mL/min.

2.3. Thermal Testing in Electric Furnace

Figure 1 shows the schematic of the thermal testing equipment. Briefly, 2 g of each sample (4 granular samples) was packed in an alumina boat and placed at the end of a quartz reaction tube. Simultaneously, gas was passed through the reaction tube, and the electric furnace (Koyo Thermo Systems Co. Ltd. KTF 035N) was heated to a given temperature. Once the rising temperature process was completed, the alumina boat was moved to the centre of the reaction tube and heated for 40 min. The heating temperature was set at 280–800˚C, the gas used was Ar or Ar-O_2 (5 mol%), and the gas flow rate was set to 100 mL/min. The exhaust gases emitted during the thermal test were collected in scrubbed bottles filled with 100 mL ultra-pure water and hexane.

2.4. Quantification of Pd, Br, and C in Solid Samples

After the thermal testing, the granular samples were pulverised using an agate mortar. Subsequently, 0.1 g of the pulverised sample and 20 mL of aqua regia were placed in a Teflon container and sealed for dissolution by microwave radiation (Analytic Jena Co., Ltd. TOPwave). Table 1 lists the sample decomposition conditions. Once dissolved, the sample was filtered, and the filtrate was diluted to 100 mL, following which Pd was quantified by inductively coupled plasma-mass spectrometry (Perkin Elmer Co., Ltd. ELAN DRC-e).

Quantification of Br and C in the solid samples was performed using an organic halogen sulphur analysis system (Yanaco Co., Ltd. YHS-11) and a micro-corder (J-Science Lab Co., Ltd. JM10), respectively.

2.5. HBr Quantification

After the thermal testing, the reaction tube was rinsed with ultra-pure water.

Table 1. Sample decomposition process conditions—microwave decomposition equipment.

	Temperature (˚C)	Heatup time (min)	Holding time (min)	Pressue (bar)
1st step	140	15	10	50
2nd step	210	10	45	50

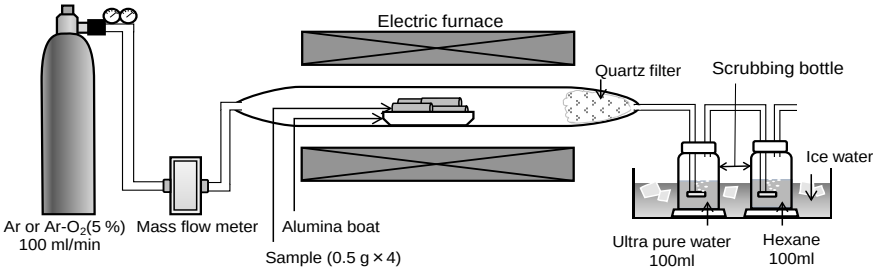

Figure 1. Overview of thermal testing equipment.

Furthermore, the quartz wool was cleaned for 1 h under ultrasonication in ultra-pure water. These cleaning fluids and ultra-pure water from the gas-scrubing bottles were filtered and diluted to 200 mL for subsequent analysis. The Br in the solution was quantified using ion chromatography (Dionex Co., Ltd. DX-120) and converted into HBr.

2.6. Crystal Structure Analysis

The crystal structure of the solid samples was determined by XRD (Bruker Co., Ltd. D8 ADVANCE/L). Table 2 lists the XRD measurement conditions.

2.7. Elemental Mapping

Elemental mapping images of the sample surface were obtained using field-emission SEM-EDS (JEOL Co., Ltd. JSM 7100F). In preparation for the SEM observations, a cross-section polisher was used to apply an Ar-ion beam sputter to the sample surface and expose the particle cross-sections.

3. Results and Discussion

3.1. Analysis of Pyrolytic and Oxidative Decomposition

Figure 2 shows the TG curves of the Pd + TBBPA and PdO + TBBPA samples and of the reagents PdO, $PdBr_2$, and TBBPA in a He atmosphere. At 200˚C, rapid weight loss was observed for the Pd + TBBPA sample, with the weight loss rate reaching 64% at 310˚C. Since this weight loss behaviour was virtually identical to that of TBBPA in this temperature range, it was believed that TBBPA volatilisation or decomposition occurred. The weight loss rate at 310˚C - 560˚C was 6.0%. Because the weight loss behaviours for PdO and $PdBr_2$ were different, this loss was probably caused by another compound. A small weight loss was also observed at 560˚C - 690˚C, but hardly any change was observed above 690˚C, with a total weight loss rate of 69% achieved by the end of the test. For the PdO + TBBPA sample, the weight loss rate was 33.9% when the temperature was increased to 310˚C. In this temperature range, the weight loss behaviour was similar to that of the Pd + TBBPA sample. However, from 350˚C to 730˚C, weight loss occurred at a nearly constant rate, differing substantially from the behaviour of the Pd + TBBPA sample. Furthermore, this weight loss behaviour did not correspond to those of the other two reagents (PdO and $PdBr_2$) in this

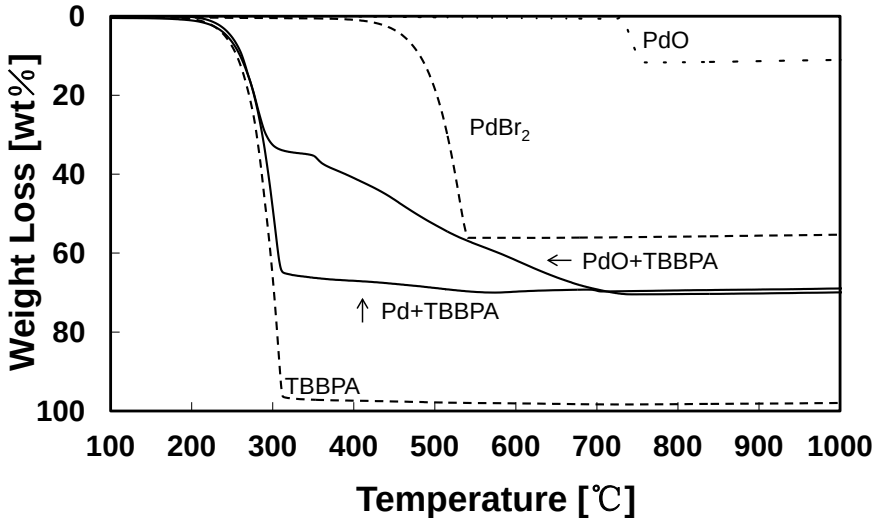

Figure 2. TG curves of Pd + TBBPA and PdO + TBBPA samples and of PdO, $PdBr_2$, and TBBPA in He atmosphere.

Table 2. XRD measurement conditions.

Voltage (kV)	40
Current (mA)	40
start angle (deg.)	10
stop angle (deg.)	80
step angle (deg.)	0.02

temperature range. The total weight loss at 730˚C was 70.3%, almost identical to that of the Pd + TBBPA sample.

Figure 3 shows the TG curves of the Pd + TBBPA sample in Ar-O_2 and He atmospheres, and the same comparison is made for the PdO + TBBPA sample in Figure 4. The TG curves for the Pd + TBBPA sample were nearly identical, and no major atmospheric-induced differences were observed. In addition, the TG curves were consistent for the PdO + TBBPA sample up to 470˚C. Subsequently, the mass of the sample gradually decreased until 730˚C in the He atmosphere and rapidly decreased until 590˚C in the Ar-O_2 atmosphere, and remained nearly constant afterwards, although slight rises and falls were observed.

3.2. Pd Bromination Accompanying TBBPA Decomposition

3.2.1. Solid/Gas Distribution of Pd, Br, and C

1) Ar atmosphere

The mass balance of Pd, C, and Br before and after heating is shown in Figure 5(a) for the Pd + TBBPA sample and in Figure 5(b) for the PdO + TBBPA sample. For the Pd + TBBPA sample, Pd volatilisation through heating was not observed. Considering the TG results (Figure 2) and the initial Pd content of 28 wt%, it could be inferred that the main residue in the sample at temperatures over 690˚C was Pd. However, the balance of C and Br was different from that of

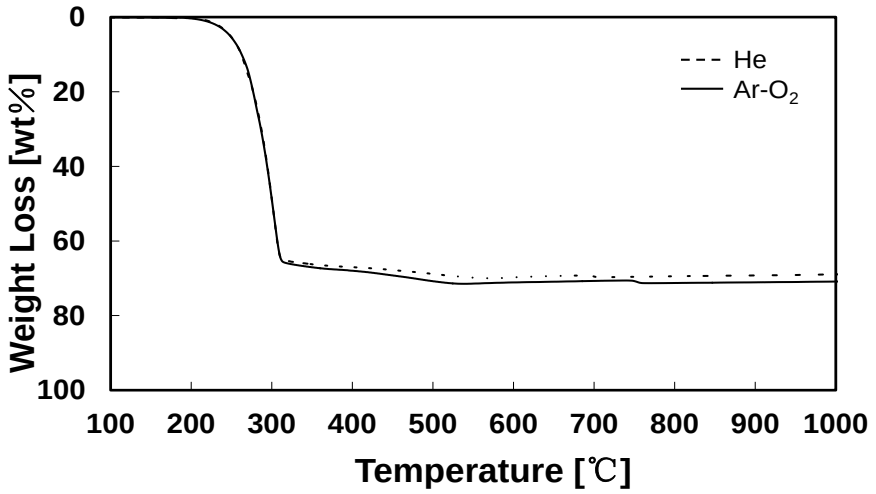

Figure 3. TG curves of Pd + TBBPA and PdO + TBBPA samples and of PdO, $PdBr_2$, and TBBPA in He atmosphere.

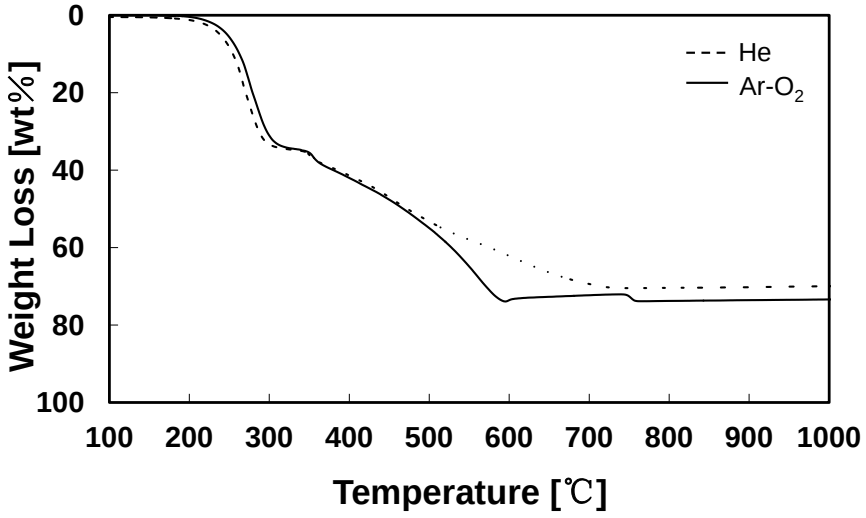

Figure 4. TG curves of PdO + TBBPA sample in Ar-O_2 and He atmospheres.

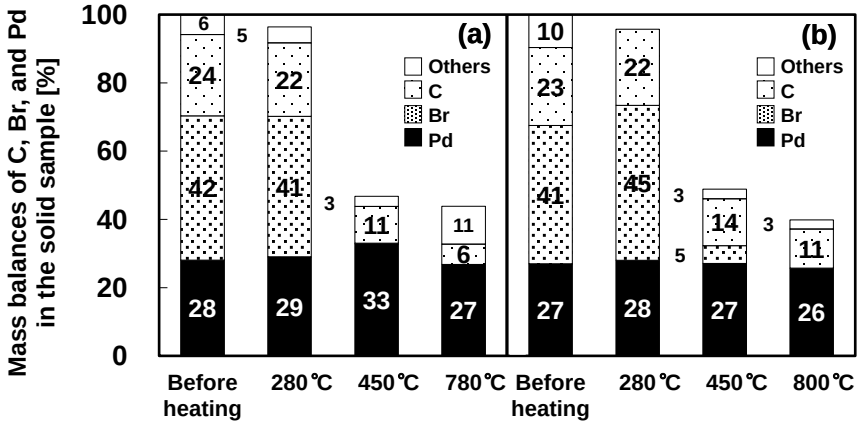

Figure 5. Pd, C, and Br mass balances before and after heating for (a) Pd + TBBPA and (b) PdO + TBBPA samples in Ar atmosphere.

Pd. The residual rates of C in the solid samples decreased with increasing temperature and the values were 89.3%, 44.3%, and 25.5% at 280˚C, 450˚C, and 780˚C, respectively. For Br, the residual rate was 96.1% at 280˚C, which decreased to 0.49% at 450˚C, and by 780˚C, Br had completely volatilised.

For the PdO + TBBPA sample, 13.0% Br residual content was observed at 450˚C, which was higher than the 0.49% content observed in the Pd + TBBPA sample. The Br volatilisation rate slowed down because of the presence of PdO, and it was surmised that decomposition occurred after Pd bromide was produced.

2) Ar-O_2 atmosphere

Pd, C, and Br balances before and after heating are shown in Figure 6(a) for the Pd + TBBPA sample and in Figure 6(b) for the PdO + TBBPA sample. The Br volatilisation rate in the Pd + TBBPA sample at 280˚C was significantly higher than that in the Ar atmosphere. No other atmospheric-induced differences were observed.

3.2.2. TBBPA to HBr Conversion Ratio

1) Ar atmosphere

Figure 7 shows the relationship between the heating temperature of the Pd + TBBPA and PdO + TBBPA samples and their respective HBr conversion rates. The HBr conversion rate of the Pd + TBBPA sample was 2.5% at 280˚C and increased to 24.7% at 450˚C. Because all Br in the solid sample volatilised at 450˚C, it was believed that HBr represented 25% of the chemical form of bromine, with the remainder occurring as Br_2 or organ bromide compounds. The HBr conversion rate was 25.6% at 780˚C, nearly identical to that at 450˚C. The HBr conversion rate in the PdO + TBBPA sample at 280˚C was low (0.7%), similar to that of the Pd + TBBPA sample. However, not only were the rates higher than those for the Pd + TBBPA sample, 63.7% at 450˚C and 72.7% at 800˚C, but they increased as a function of temperature. This indicated that TBBPA thermal decomposition differed substantially in the presence of Pd and PdO.

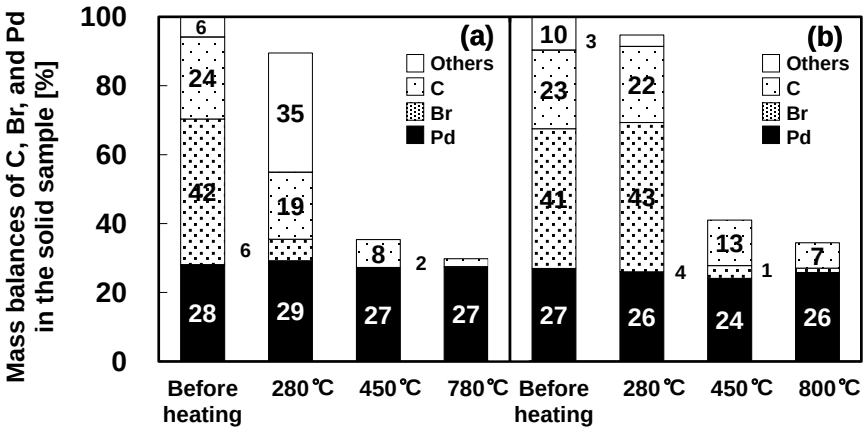

Figure 6. Pd, C, and Br mass balances before and after heating for (a) Pd + TBBPA and (b) PdO + TBBPA samples in Ar-O_2 atmosphere.

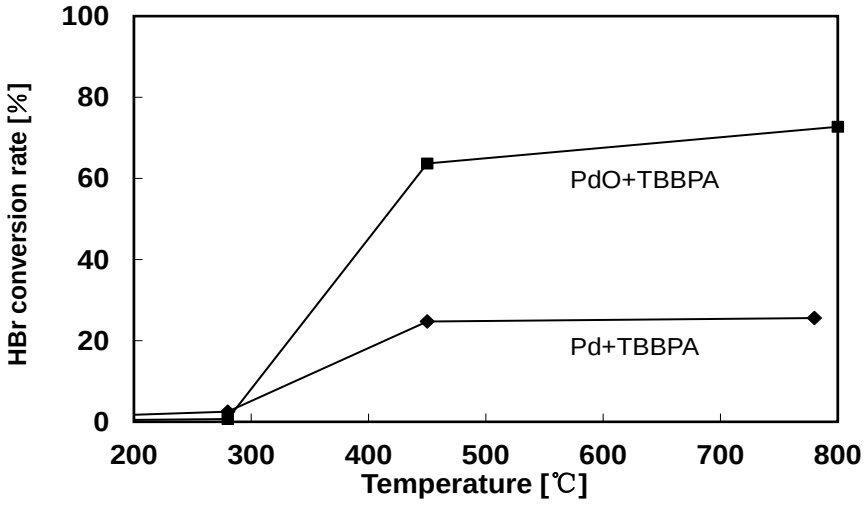

Figure 7. Pd, C, and Br mass balances before and after heating for (a) Pd + TBBPA and (b) PdO + TBBPA samples in Ar-O_2 atmosphere.

2) Ar-O_2 atmosphere

Figure 8 shows the relationship between heating temperatures of the Pd + TBBPA and PdO + TBBPA samples and their respective HBr conversion rates. The HBr conversion rates for the Pd + TBBPA sample were 1.4% and 30.7% at 280 and 450˚C, respectively. The rate substantially increased to 67.2% at 780˚C (nearly twice) in an inert atmosphere. This indicated that when Pd was present, oxygen in the atmosphere promoted HBr conversion in TBBPA.

The HBr conversion rates in the PdO + TBBPA sample were 51.6% and 57.4% at 450 and 800˚C, respectively, with higher values in the inert atmosphere under identical temperature conditions. When PdO was present, HBr conversion rates were lower than that in the inert atmosphere at temperatures greater than 450˚C due to the presence of oxygen, and the impact on Br_2 production was likely substantial.

3.2.3. Crystal Structure Analysis Using XRD

1) Ar atmosphere

Figure 9(a) and Figure 9(b) show the XRD patterns for the Pd + TBBPA and PdO + TBBPA samples, respectively. For the Pd + TBBPA sample, at 280˚C, in addition to a clear Pd peak, peaks arising from TBBPA and its decomposition products were observed in the 2θ range 10.4˚ - 38.3˚. However, at 450˚C and higher, only Pd peaks were detected.

For the PdO + TBBPA sample, at 280˚C, peaks originating from TBBPA decomposition products could be observed at 2θ = 14.0˚ and 22.7˚ - 24.1˚. Furthermore, both PdO and Pd peaks were detected. Since the thermal decomposition of PdO to Pd occurred at 750˚C or higher (Figure 2), PdO reduction reactions with TBBPA decomposition products occurred. The PdO peaks disappeared at 450˚C and 800˚C, and only Pd peaks could be confirmed.

2) Ar-O_2 atmosphere

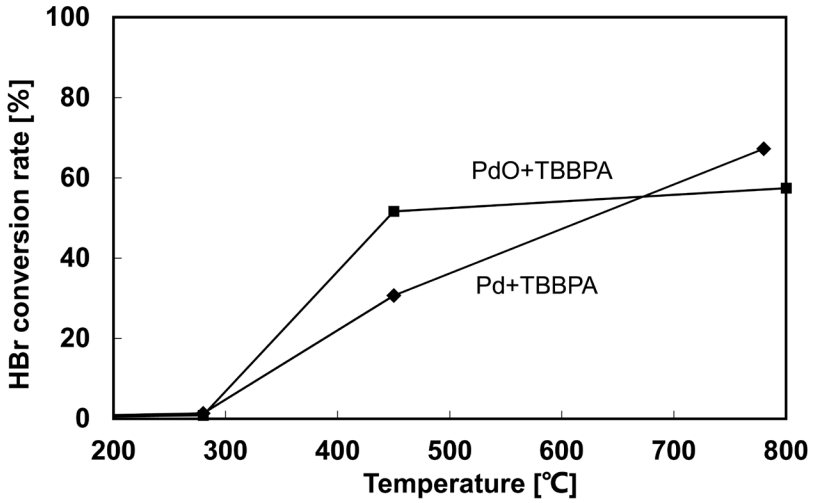

Figure 8. Relation between heating temperature and HBr conversion rate in Pd + TBBPA and PdO + TBBPA samples in Ar-O_2 atmosphere.

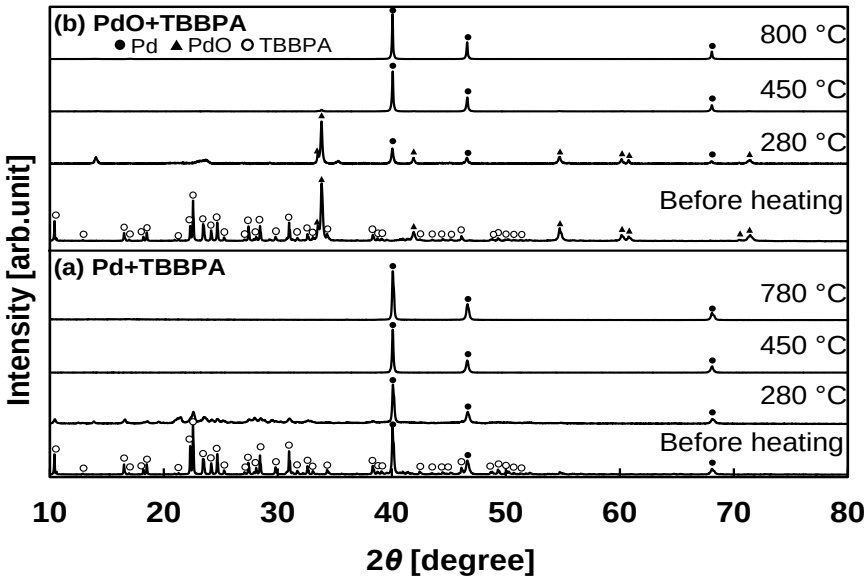

Figure 9. XRD patterns of (a) Pd + TBBPA and (b) PdO + TBBPA samples in Ar atmosphere.

Figure 10(a) and Figure 10(b) show the XRD patterns for the Pd + TBBPA and PdO + TBBPA samples, respectively. The peaks originating from the TBBPA decomposition products and Pd were observed for the Pd + TBBPA sample at 280˚C. Similar to observations in the Ar atmosphere, only Pd peaks were detected at 450 or 780˚C. The XRD patterns of the PdO + TBBPA sample were similar to those obtained in the Ar atmosphere, and no significant atmospheric-induced differences were observed in terms of the chemical form of Pd.

3.2.4. Pd and Br Elemental Mapping

1) Ar Atmosphere

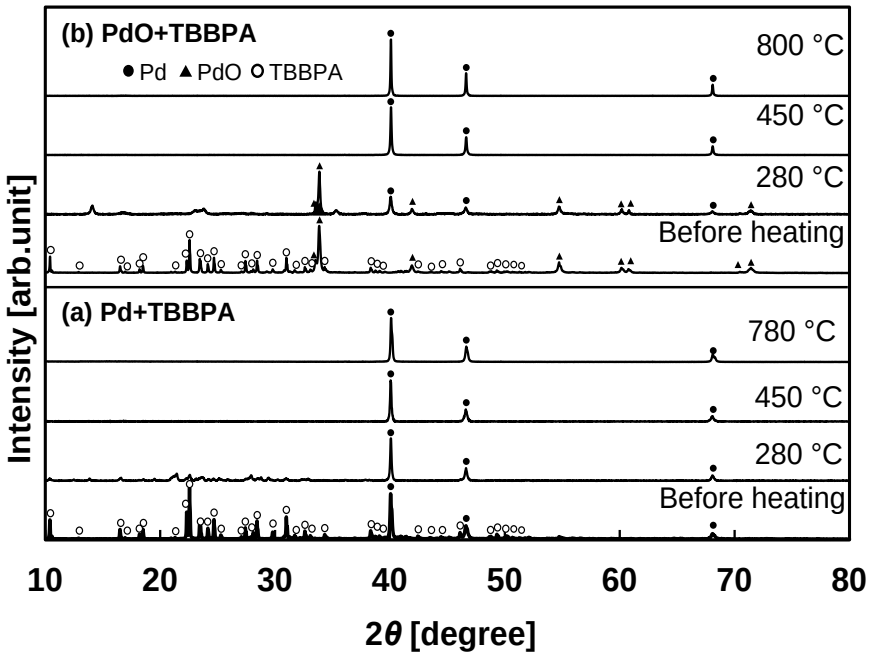

Figure 10. XRD patterns of (a) Pd + TBBPA and (b) PdO + TBBPA samples in Ar-O_2 atmosphere.

Figure 11(a) and Figure 11(b) show the SEM images and Pd and Br elemental mapping of the Pd + TBBPA and PdO + TBBPA samples, respectively, before and after heating. Table 3 lists the semi-quantitative analysis results for Pd and Br obtained by SEM-EDS. The presence of Pd and Br was clearly confirmed in the Pd + TBBPA sample before heating and at 280˚C, although the images did not perfectly overlap. Br was believed to exist primarily in the form of an organic compound, which was consistent with the XRD results (Figure 9(a)). However, only Pd was observed at temperatures greater than 450˚C.

For the PdO + TBBPA sample, at 280˚C, no significant difference with respect to the Pd + TBBPA sample was observed in the Pd and Br mapping images. However, in addition to the comparatively high concentration of Br (7.3%) at 450˚C, partial overlap of Pd and Br was observed. This suggested that Pd bromide compounds were present, and that Pd bromination reactions occurred between 280˚C and 450˚C. As shown in the TG curves (Figure 2), weight loss occurred at a nearly constant rate between 350˚C and 730˚C, which was likely caused by bromide decomposition. This was confirmed by the absence of Br at 800˚C and the sole presence of Pd.

2) Ar-O_2 Atmosphere

Figure 12(a) and Figure 12(b) show the SEM images and Pd and Br elemental mapping images of the Pd + TBBPA and PdO + TBBPA samples, respectively, before and after heating. Table 4 lists the semi-quantitative analysis results for Pd and Br obtained by SEM-EDS. Similar to the results in the Ar atmosphere, Pd and Br were present at 280˚C, although the mapping images did not overlap. Furthermore, no Br was observed at 450˚C or 780˚C.

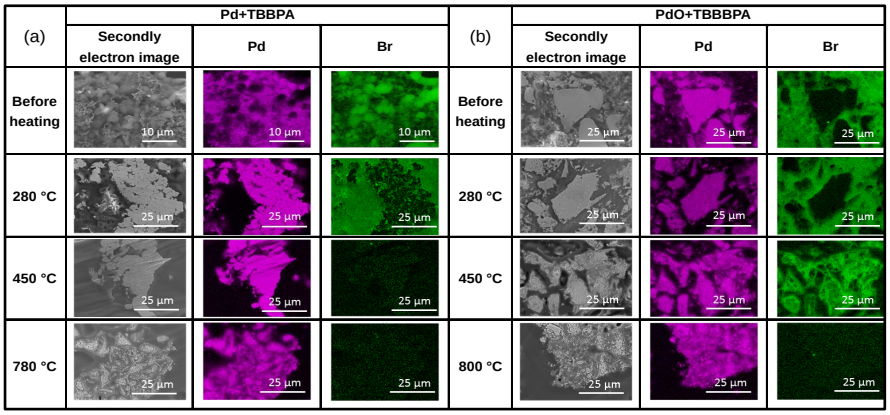

Figure 11. SEM images and Pd/Br elemental mapping images before and after heating for (a) Pd + TBBPA and (b) PdO + TBBPA in Ar atmosphere.

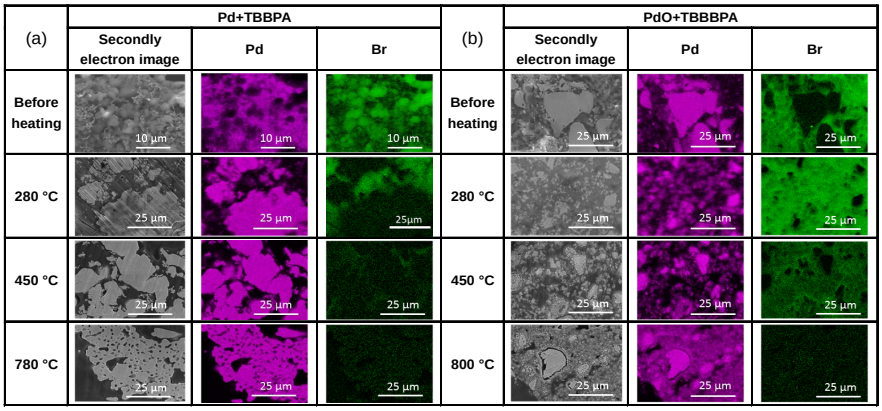

Figure 12. SEM images and Pd/Br elemental mapping images before and after heating for (a) Pd + TBBPA and (b) PdO + TBBPA in Ar-O_2 atmosphere.

Table 3. Semi-quantitative analysis results for Pd and Br concentrations using SEM-EDS in Ar atmosphere.

		Pd (wt%)	Br (wt%)
Pd + TBBPA	Before Heating	48	10
	280˚C	49	4
	450˚C	27	0.05
	780˚C	32	0.07
PdO + TBBPA	Before Heating	41	9.3
	280˚C	30	30
	450˚C	32	7.3
	800˚C	33	0.15

Although Pd and Br were present up to 280˚C in the PdO + TBBPA sample, no overlap of the mapping images was observed. The Br concentration was 5.0% at 450˚C, but no areas were observed with a clear overlap of Pd and Br mapping images. As in the inert atmosphere, only Pd was detected at 800˚C.

Table 4. Semi-quantitative analysis results for Pd and Br concentrations using SEM-EDS in Ar-O_2 atmosphere.

		Pd (wt%)	Br (wt%)
Pd + TBBPA	Before Heating	48	10
	280˚C	48	1.4
	450˚C	64	0.4
	780˚C	61	0.14
PdO + TBBPA	Before Heating	41	9.3
	280˚C	16	36
	450˚C	34	5.0
	800˚C	50	0.26

4. Conclusions

In this study, thermal testing of TBBPA and Pd/PdO mixtures (Pd + TBBPA and PdO + TBBPA) was conducted to study the chemical form of Pd obtained during TBBPA pyrolytic and oxidative decomposition and combustion.

In the pyrolytic test of the Pd + TBBPA sample, Pd bromination did not occur. Furthermore, Pd primarily existed as a metal, regardless of the temperature conditions or the presence of oxygen. In the PdO + TBBPA sample, SEM-EDS indicated that Pd bromide was present in the solid samples obtained in an Ar atmosphere at 450˚C. The absence of Pd bromide at 280˚C suggested that the bromination reaction occurred at 280˚C - 450˚C. Weight loss occurred at an almost constant rate, as indicated by TG-DTA, between 350˚C and 730˚C, indicating that Pd bromide decomposed in this temperature range.

Acknowledgements

This work was supported by JSPS KAKENHI Grant Number 16K00664, and by the Cooperative Research Program of "Network Joint Research Center for Materials and Devices," and by the High Efficiency Rare Elements Extraction Technology Area in the Tohoku Innovation Materials Technology Initiatives for Reconstruction from the Ministry of Education, Culture, Sports, Science and Technology in Japan.

References

[1] Ogunseitan, A.O. (2013) The Basel Convention and e-Waste: Translation of Scientific Uncertainty to Protective Policy. *The Lancet Global Health*, **1**, 313-314. https://doi.org/10.1016/S2214-109X(13)70110-4

[2] Huang, K., Guo, J. and Xu, Z. (2009) Recycling of Waste Printed Circuit Boards: A Review of Current Technologies and Treatment Status in China. *Journal of Hazardous Materials*, **164**, 399-408. https://doi.org/10.1016/j.jhazmat.2008.08.051

[3] Cui, J. and Forssberg, E. (2007) Characterisation of Shredded Television Scrap and Implications for Materials Recovery. *Waste Management*, **27**, 415-424. https://doi.org/10.1016/j.wasman.2006.02.003

[4] Ilyas, S., Anwar, M., Niazi, S.B. and Ghauri, M.A. (2007) Bioleaching of Metals from Electronic Scrap by Moderately Thermophilic Acidophilic Bacteria. *Hydrometallurgy*, **88**, 180-188. https://doi.org/10.1016/j.hydromet.2007.04.007

[5] Christian, H. (2006) Recycling of Electronic Scrap at Umicore's Integrated Metals Smelter and Refinery. *World of Metallurgy—ERZMETALL*, **59**, 152-161.

[6] Yang, H., Liu, J. and Yang, J. (2011) Leaching Copper from Shredded Particles of Waste Printed Circuit Boards. *Journal of Hazardous Materials*, **187**, 393-400. https://doi.org/10.1016/j.jhazmat.2011.01.051

[7] Oh, C.J., Lee, S.O., Yang, H.K., Ha, T.J. and Kim, M.J. (2003) Selective Leaching of Valuable Metals from Waste Printed Circuit Boards. *Journal of the Air & Waste Management Association*, **53**, 897-902. https://doi.org/10.1080/10473289.2003.10466230

[8] Oleszek, S., Grabda, M., Shibata, E. and Nakamura, T. (2013) Distribution of Copper, Silver and Gold during Thermal Treatment with Brominated Flame Retardants. *Waste Management*, **33**, 1835-1842. https://doi.org/10.1016/j.wasman.2013.05.009

[9] Yang, Y., Chen, S., Li, S., Chen, M., Chen, H. and Liu, B. (2014) Bioleaching Waste Printed Circuit Boards by Acidithiobacillus Ferrooxidans and Its Kinetics Aspect. *Journal of Biotechnology*, **173**, 24-30. https://doi.org/10.1016/j.jbiotec.2014.01.008

[10] Xiu, F.-R., Weng, H., Qi, Y., Yu, G., Zhang, Z. and Zhang, F.-S. (2016) A Novel Reutilisation Method for Waste Printed Circuit Boards as flame Retardant and Smoke Suppressant for poly (vinyl chloride). *Journal of Hazardous Materials*, **315**, 102-109. https://doi.org/10.1016/j.jhazmat.2016.04.076

[11] Xiu, F.-R. and Zhang, F.-S. (2010) Materials Recovery from Waste Printed Circuit Boards by Supercritical Methanol. *Journal of Hazardous Materials*, **178**, 628-634. https://doi.org/10.1016/j.jhazmat.2010.01.131

[12] Duan, C.L., Diao, Z.J., Zhao, Y.M. and Huang, W. (2015) Liberation of Valuable Materials in Waste Printed Circuit Boards by High-Voltage Electrical Pulses. *Minerals Engineering*, **70**, 170-177. https://doi.org/10.1016/j.mineng.2014.09.018

[13] Serpe, A., Artizzu, F., Mercuri, M.L., Pilia, L. and Deplano, P. (2008) Charge Transfer Complexes of Dithioxamides with Dihalogens as Powerful Reagents in the Dissolution of Noble Metals. *Coordination Chemistry Reviews*, **252**, 1200-1212. https://doi.org/10.1016/j.ccr.2008.01.024

[14] Ortuño, N., Moltó, J., Conesa, J.A. and Font, R. (2014) Formation of Brominated Pollutants during the Pyrolysis and Combustion of Tetrabromobisphenol A at Different Temperatures. *Environmental Pollution*, **191**, 31-37. https://doi.org/10.1016/j.envpol.2014.04.006

[15] Lin, K.-H. and Chiang, H.-L. (2014) Liquid Oil and Residual Characteristics of Printed Circuit Board Recycle by Pyrolysis. *Journal of Hazardous Materials*, **271**, 258-265. https://doi.org/10.1016/j.jhazmat.2014.02.031

[16] Chiang, H.-L. and Lin, K.-H. (2014) Exhaust Constituent Emission Factors of Printed Circuit Board Pyrolysis Processes and Its Exhaust Control. *Journal of Hazardous Materials*, **264**, 545-551. https://doi.org/10.1016/j.jhazmat.2013.10.049

[17] Han, S.-K., Bilski, P., Karriker, B., Sik, R.H. and Chignell, C.F. (2008) Oxidation of Flame Retardant Tetrabromobisphenol A by Singlet Oxygen. *Environmental Science & Technology*, **42**, 166-172. https://doi.org/10.1021/es071800d

[18] Blazsó, M. and Czégény, Z. (2006) Catalytic Destruction of Brominated Aromatic Compounds Studied in a Catalyst Microbed Coupled to Gas Chromatography/Mass Spectrometry. *Journal of Chromatography A*, **1130**, 91-96. https://doi.org/10.1016/j.chroma.2006.05.009

[19] Luda, M.P., Balabanovich, A.I., Hornung, A. and Camino, G. (2003) Thermal Degradation of a Brominated Bisphenol A Derivative. *Polymers for Advanced Technologies*, **14**, 741-748. https://doi.org/10.1002/pat.389

[20] Chien, Y.-C., Wang, H.P., Lin, K.S., Huang, Y.-J. and Yang, Y.W. (2000) Fate of Bromine in Pyrolysis of Printed Circuit Board Wastes. *Chemosphere*, **40**, 383-387. https://doi.org/10.1016/S0045-6535(99)00251-9

[21] Liu, W.-J., Tian, K., Jiang, H. and Yu, H.-Q. (2016) Lab-Scale Thermal Analysis of Electronic Waste Plastics. *Journal of Hazardous Materials*, **310**, 217-225. https://doi.org/10.1016/j.jhazmat.2016.02.044

[22] Matsuura, H. and Tsukihashi, F. (2006) Chlorination Kinetics of ZnO with Ar-Cl_2-O_2 Gas and the Effect of Oxychloride Formation. *Metallurgical and Materials Transactions B*, **37**, 413-420. https://doi.org/10.1007/s11663-006-0026-7

[23] Matsuura, M., Hamano, T. and Tsukihashi, F. (2006) Chlorination Kinetics of $ZnFe_2O_4$ with Ar-Cl_2-O_2 Gas. *Materials Transactions*, **47**, 2524-2532.

[24] Zhang, B., Yan, X.-Y., Shibata, K., Uda, T., Tada, M. and Hirasawa, M. (2000) Thermogravimetric-Mass Spectrometric Analysis of the Reactions between Oxide (ZnO, Fe_2O_3 or $ZnFe_2O_4$) and Polyvinyl Chloride under Inert Atmosphere. *Materials Transactions*, **41**, 1342-1350.

[25] Grabda, M., Oleszek-Kudlak, S., Shibata, E. and Nakamura, T. (2011) Vaporisation of Zinc during Thermal Treatment of ZnO with Tetrabromobisphenol A (TBBPA). *Journal of Hazardous Materials*, **187**, 473-479. https://doi.org/10.1016/j.jhazmat.2011.01.060

[26] Shibata, E., Grabda, M. and Nakamura, T. (2006) Thermodynamic Consideration of the Bromination Reactions of Inorganic Compound—Considerations of Flame-Retardant Mechanisms and Degradation Recycling of Brominated Flame Retardant Plastics. *Journal of the Japan Society of Waste Management Experts*, **17**, 361-371.

[27] Oleszek, S., Grabda, M., Shibata, E. and Nakamura, T. (2012) TG and TG-MS Methods for Studies of the Reaction between Metal Oxide and Brominated Flame Retardant in Various Atmospheres. *Thermochimica Acta*, **527**, 13-21. https://doi.org/10.1016/j.tca.2011.09.014

[28] Grabda, M., Oleszek-Kudlak, S., Shibata, E. and Nakamura, T. (2009) Influence of Temperature and Heating Time on Bromination of Zinc Oxide during Thermal Treatment with Tetrabromobisphenol A. *Environmental Science & Technology*, **43**, 8936-8941. https://doi.org/10.1021/es901845m

[29] Grabda, M., Oleszek-Kudlak, S., Rzyman, M., Shibata, E. and Nakamura, T. (2009) Studies on Bromination and Evaporation of Zinc Oxide during Thermal Treatment with TBBPA. *Environmental Science & Technology*, **43**, 1205-1210. https://doi.org/10.1021/es802400y

[30] Oleszek, S., Grabda, M., Shibata, E. and Nakamura, T. (2013) Fate of Lead Oxide during Thermal Treatment with Tetrabromobisphenol A. *Journal of Hazardous Materials*, **261**, 163-171. https://doi.org/10.1016/j.jhazmat.2013.07.028

[31] Oleszek, S., Grabda, M., Shibata, E. and Nakamura, T. (2013) Study of the Reactions between Tetrabromobisphenol A and PbO and Fe_2O_3 in Inert and Oxidizing Atmospheres by Various Thermal Methods. *Thermochimica Acta*, **566**, 218-225. https://doi.org/10.1016/j.tca.2013.06.003

[32] Rzyman, M., Grabda, M., Oleszek-Kudlak, S., Shibata, E. and Nakamura, T. (2010) Studies on Bromination and Evaporation of Antimony Oxide during Thermal Treatment of Tetrabromobisphenol A (TBBPA). *Journal of Analytical and Applied*

Pyrolysis, **88**, 14-21. https://doi.org/10.1016/j.jaap.2010.02.004

[33] Grabda, M., Oleszek, S., Shibata, E. and Nakamura, T. (2014) Study on Simultaneous Recycling of EAF Dust and Plastic Waste Containing TBBPA. *Journal of Hazardous Materials*, **278**, 25-33. https://doi.org/10.1016/j.jhazmat.2014.05.084